Materials Science Forum Vols. 768-769 (2014) pp 433-440
Online available since 2013/Sep/23 at www.scientific.net

doi:10.4028/www.scientific.net/MSF.768-769.433

Through-Thickness Stresses in Automotive Sheet Metal after Plane Strain Channel Draw

Thomas Gnäupel-Herold[1, a], Daniel E. Green[2,b], Timothy Foecke[3,c] and Mark A. Iadicola[3,d]

[1]NIST Center for Neutron Research, 100 Bureau Dr. M/S 6102 Gaithersburg, MD 20899-6102, USA

[2]University of Windsor, Department of Mechanical, Automotive & Materials Engineering, Windsor, Ontario N9B 3P4, Canada

[3]NIST Center for Automotive Lightweighting, 100 Bureau Drive, M/S 8553

Gaithersburg, MD 20899-8553

[a]tg-h@nist.gov, [b]dgreen@uwindsor.ca, [c]timothy.foecke@nist.gov, [d]mark.iadicola@nist.gov

Keywords: Sheet Metal Stress; Plane Strain Stretch Bending; Diffraction; Springback; Forming.

Abstract. A series of samples from four automotive materials - AKDQ, HSLA50, DP600, and AA6022-T43 - were deformed in a channel draw processes with different levels of draw bead penetration. As a result, varying magnitudes of deformations in plane strain mode and residual stresses were obtained. Through-thickness stress profiles were obtained non-destructively using a novel, high resolution X-ray diffraction technique.

Introduction

In automotive sheet metal forming the deployment of newer, high-strength materials for automotive applications is inextricably linked to the predictability of multi-axial forming behavior, particularly forming limits and final shape. The latter is a direct result of springback and therefore the result of the residual stress profile that arises from inhomogeneous through-thickness plastic strains. Springback is known for the considerable cost it causes in the tryout phase for forming tool development. This problem is exacerbated through light-weighting constraints which force either thickness reduction with increased yield strength (steels) or altogether lighter materials (aluminum alloys) which typically have larger yield to elastic modulus ratios. All these effects increase the springback to varying degrees. Efforts for springback prediction generally focus on single number comparison, i.e. the comparison of a measured and predicted deflection angle or displacement. However, it is important to remember that springback is the result of balancing bending moments which are the result of residual stresses. Thus, the comparison of the through-thickness stress profiles from calculation and measurement can be a valuable tool in refining the underlying material model for the calculation. However, such a measurement represents an experimental challenge because of the minimum number of stress values necessary to describe the through-thickness profile. Typical sheet thicknesses are 1 mm or less and this places high demands on the spatial resolution of stress determination. Past efforts on select samples have focused on using neutron diffraction [1,2] and synchrotron X-ray diffraction [3,4] where spatial resolutions of ≈0.1 mm..0.3 mm have been achieved. However, some measurements such as in [1] were fraught with problems stemming from insufficient spatial resolution and unsuitable measurement locations. For example, there were apparent stress balance violations and large uncertainties due to low neutron intensity. A recently developed X-ray method [5] provides easier access at resolutions similar to synchrotron X-ray diffraction, thus allowing the study of a larger number both of materials and forming parameters. The results presented here were obtained from X-ray measurements on samples of four different materials (AKDQ, HSLA50, DP600, and AA6022) deformed in a channel draw at different draw bead penetrations.

Experimental

Material. The details and the purpose of the channel draw as well as materials property data for AKDQ, HSLA 50, DP 600, and AA6022-T43, were presented in earlier publications [1,6], thus only an outline is given. The channel draw investigated here produced samples deformed in the plane strain mode, i.e. samples were stretched in the sheet transverse direction (TD) only (from $\varepsilon_{TD} \approx 0.05$ at 25 % draw bead penetration up to $\varepsilon_{TD} \approx 0.15$ at 100 % penetration) with shrinkage strain only in the thickness ($\varepsilon_{ND} < 0$; $\varepsilon_{RD} \approx 0$).

The forming geometry is shown in Fig. 1. A number of steps were necessary to produce samples suitable for X-ray diffraction. The side panels were trimmed, and smaller specimens (x=25 mm, y=12 mm, z≤1 mm) were removed at ≈15 mm distance from the rim by means of electro-discharge machining. The specimens were cast in a block of epoxy and their cross section surfaces polished to remove all influence of the EDM cutting (total removal ≈ 1 mm). The final polishing step was a 0.05 μm SiC suspension intended to provide a surface undisturbed by mechanical damage other than the forming process. Fig. 2 shows the final assembly of samples for X-ray diffraction. The dimensions of the specimens were > 10 × thickness, and it is a reasonable assumption that the stresses were left undisturbed by the removal procedure.

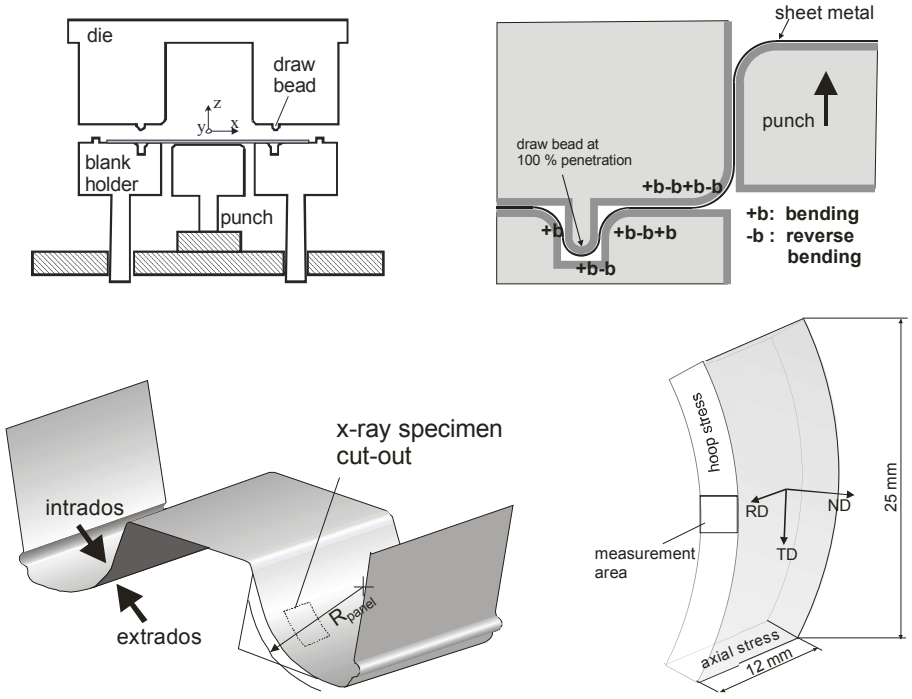

Figure 1. Top, left: setup of the channel draw process [1,6], sequences of bending and reverse bending (top, right). Bottom, left: final specimen with the X-ray sample cut-out (right, enlarged).

Diffraction Measurements. Through-thickness stresses are not an obvious subject of X-ray (surface limited) stress measurements. The choice for measuring such sub-surface stresses is usually to use a bulk-penetrating neutron or synchrotron X-ray technique as discussed in [1-4]. However, if one assumes that the deformation is homogeneous along RD and TD, then the extraction of a smaller coupon (lateral dimensions 12× and 25× thickness) will preserve the stress fields of interest. Moreover, the same stresses are "visible" on the cross section surface as shown in Fig. 2, left. The associated strains can be measured using X-ray diffraction provided that diffracted intensity can be measured on a sufficiently small area commensurate with the required depth resolution. This was carried out using the technique described in [5] which is based on keeping a small (here: 0.05 mm x 2.5 mm) X-ray beam both at a fixed sample location and a fixed beam spot orientation (Fig. 2).

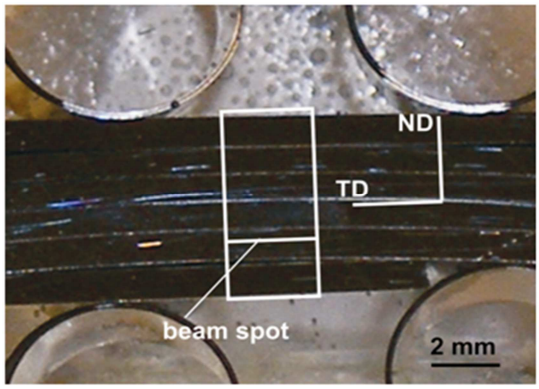

Figure 2. Side surfaces of four stacked sheet metal samples (top and bottom are backing plates). The white rectangle is the area to which the X-ray beam is confined. The beam spot stays in the orientation shown (|| TD) through all rotations (φψ). The d-spacings at the next "depth" are measured by translating along ND with an effective resolution of 0.05 mm.

Shown in Fig. 3, the central principle of this method is that the specimen rotations (φψ) cause a virtual rotation of the beam spot on the sample surface. In order to re-align the beam spot with a principal sample direction the specimen must be counter-rotated (angle δ) about the axis perpendicular to the sample surface (specimen: axis $\mathbf{z_s}$; diffractometer: axis $\boldsymbol{\varphi}\|\ \mathbf{z_s}$). For symmetric diffraction (incident and diffracted beam have the same angle to the surface normal), the angle δ is

$$\delta = \pm \arccos\left(\frac{\sin\psi \sin\theta + \cos\psi \cot\psi \sin\theta}{\sqrt{\cos^2\theta + \left(\sin\psi \sin\theta + \cos\psi \cot\psi \sin\theta\right)^2}} \right). \quad (1)$$

Here, θ is the Bragg angle, φ is the rotation about $\mathbf{z_s}$, and ψ is the tilt angle.

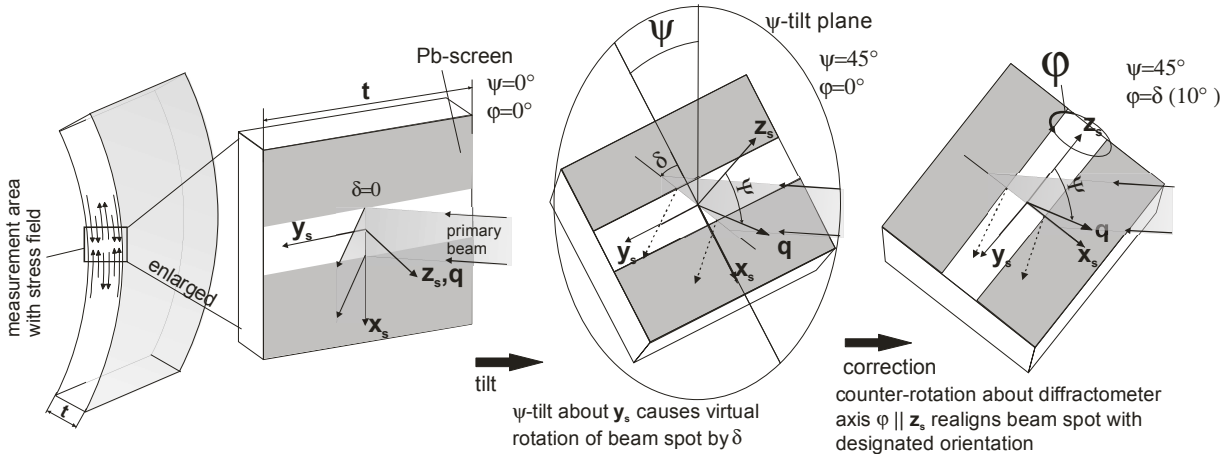

Figure 3.Virtual rotation of the beam spot (line) on the sample with ψ. At ψ=0° the strain component parallel $\mathbf{z_s}$ is measured while at φ=0, ψ=90° the strain component parallel to $\mathbf{x_s}$ is measured. One has TD=$\mathbf{x_s}$ (hoop), ND=$\mathbf{y_s}$ (radial), and RD=$\mathbf{z_s}$ (axial).

In practice, each d-measurement is done at a different (φ,ψ) combination, i.e. even φ has a slight variation. Fig. 4. shows a more familiar plot as a sheet metal pole figure with the measurement angles denoted in the pole figure reference system.

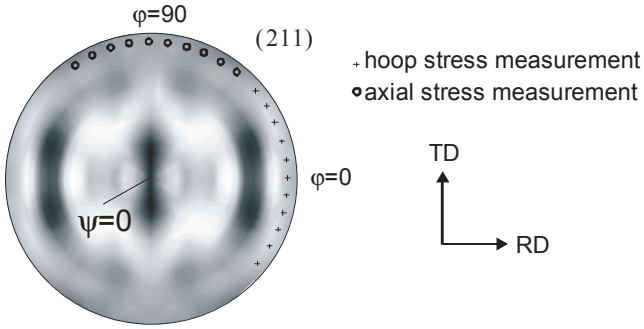

Figure 4. Angular positions of measurements plotted on a HSLA 50 pole figure (25% penetration) of the (211) reflection.

The boundary condition of a fixed orientation of the beam spot (line shape) on the sample surface requires both the Euler geometry of rotation and XYZ positioning of the sample. The equipment used is shown in Fig. 5.

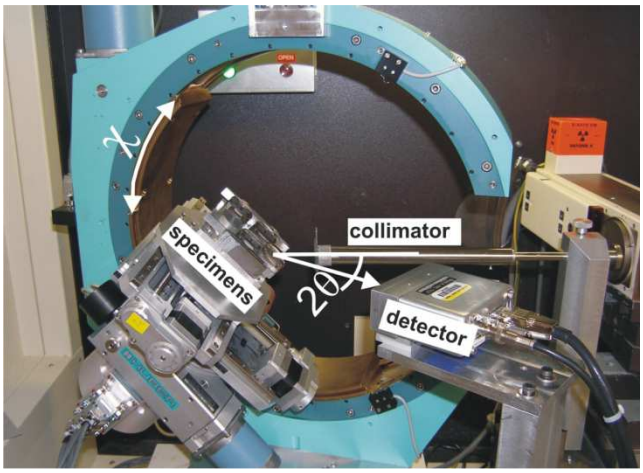

Figure 5. Euler geometry X-ray diffractometer used for the measurements discussed here.

Intergranular Strains and Texture. Due to the large plastic strains in the channel draw both intergranular (IG) strains and elastic anisotropy of diffraction elastic constants are of concern. Texture was measured for each material at the 25 % penetration and 100 % penetration level, and the orientation distribution functions (ODF) were evaluated. ODFs at intermediate penetrations (75 % and 100 %) were obtained through linear interpolation between the ODF at 25 % and the ODF at 100 %. The ODFs were subsequently used for the calculation of the (hkl, φ,ψ) dependent diffraction elastic constants using IsoDEC [9].

Several steps were taken for suppressing the effect of IG strains on the stress evaluation: 1) at least two reflections (hkl) were measured and averaged (steel: (211) and (310); AA6022: (311), (331), (420)) stress balance and momentum balance were applied to the intermediate results of the stress evaluation (Fig. 6). More specifically, a constant is added such that stress balance ($\iint \sigma_{xx} dydz = 0$) is obtained, and a depth-proportional stress is added to obtain balance of bending moments ($\int_{-t/2}^{t/2} -y\ \sigma_{xx} dy = 0$).

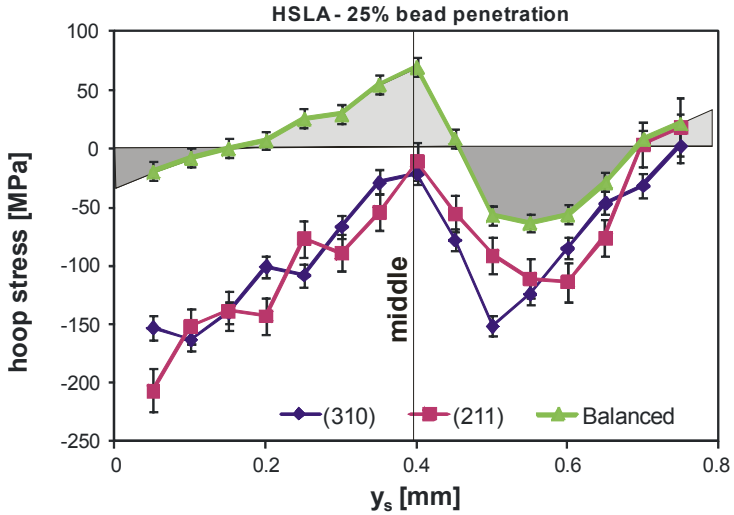

Figure 6. Stresses determined from the as-measured strains for the (211) and (310) reflections of HSLA50, 25 % bead penetration. The label 'balanced' refers to the enforced conditions of stress and momentum balance.

There are several potential problems in applying these corrections. While the applicability of both momentum balance and stress balance is without question, any non-linear ($\sin^2\psi$) through-thickness dependence of intergranular strains cannot be addressed this way. However, the compounded effect of intergranular strains is accessible through thickness-averaging, i.e. d-spacings for a given combination of (hkl, φ,ψ) are averaged over thickness (Fig. 7).

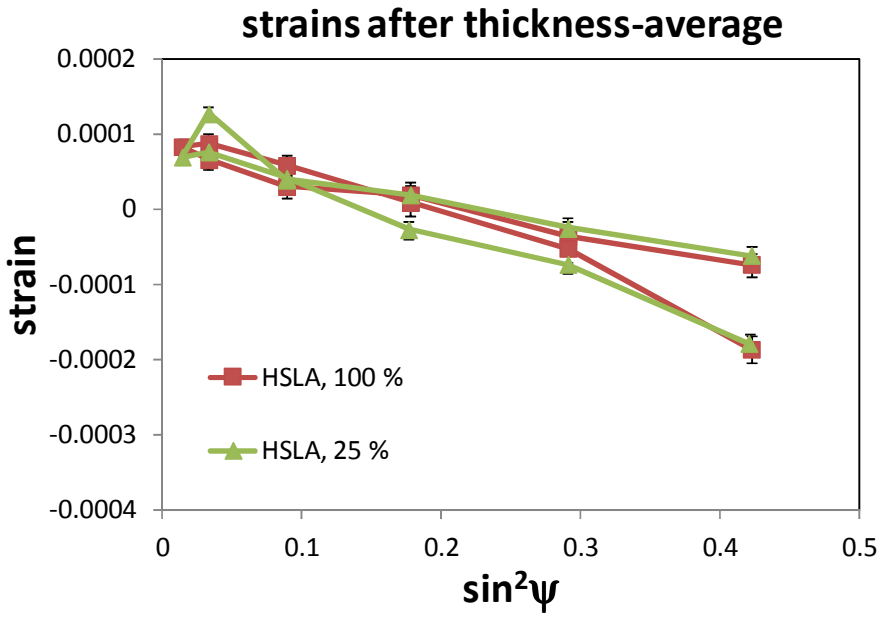

Figure 7. Through-thickness average of ε((211), φ,ψ) which essentially represents the average intergranular strains. The conversion from d((211), φ,ψ) to ε was done using the global average of all measured d as reference.

The slope of ε($\sin^2\psi$) in Fig. 6 can be interpreted as the average intergranular stress. This average stress value is subtracted from the depth dependent stresses to obtain stress balance (see Fig. 6, the (310) and (211) curves are shifted upwards by ≈80 MPa). For all materials and penetrations the momentum balance is consistently violated such that starting at intrados stresses are too far in the compressive region, thus giving all stresses (for all materials and penetrations) the characteristic tilted shape shown in Fig. 6 both for the (211) and (310) reflections. It can be surmised that this "compressive" contribution diminishes with increasing depth. In lack of other experimental data the intergranular stress contribution is therefore approximated through the aforementioned linear function.

Results and Discussion

The stresses obtained by the procedures described above are summarily shown in Fig. 8. Due to the similarities in the forming processes, the qualitative distribution of stresses are similar as well. However, the principal shape of the stress distributions is determined less by the overall plastic strains (major strains between 0.05 and 0.2 in the extreme). The stretching produces plastic strain that is homogeneous through thickness, and it would not create residual stresses by itself. On the other hand, non-homogeneous through-thickness strain is produced by the sequence of bending and reversed bending as depicted schematically in Fig. 1. The bending sequence is the same for all samples, and it is responsible for the wave-like shape of the stresses vs. depth. Moreover, a survey of residual stresses from sheet metal forming operations reported in the literature shows the same wave-like distribution through thickness almost regardless of the combination of major strain and minor strain. For example, in the deep drawn cup / split-ring test [10] one has for the through-thickness average strains $\varepsilon_{axial} \approx -\varepsilon_{hoop}$ (overall strains, overall > 0.2) while in pure bending one has $\varepsilon_{axial} \approx \varepsilon_{hoop} \approx 0$ and yet the residual stresses are very similar. Both examples are shown in Fig. 9.

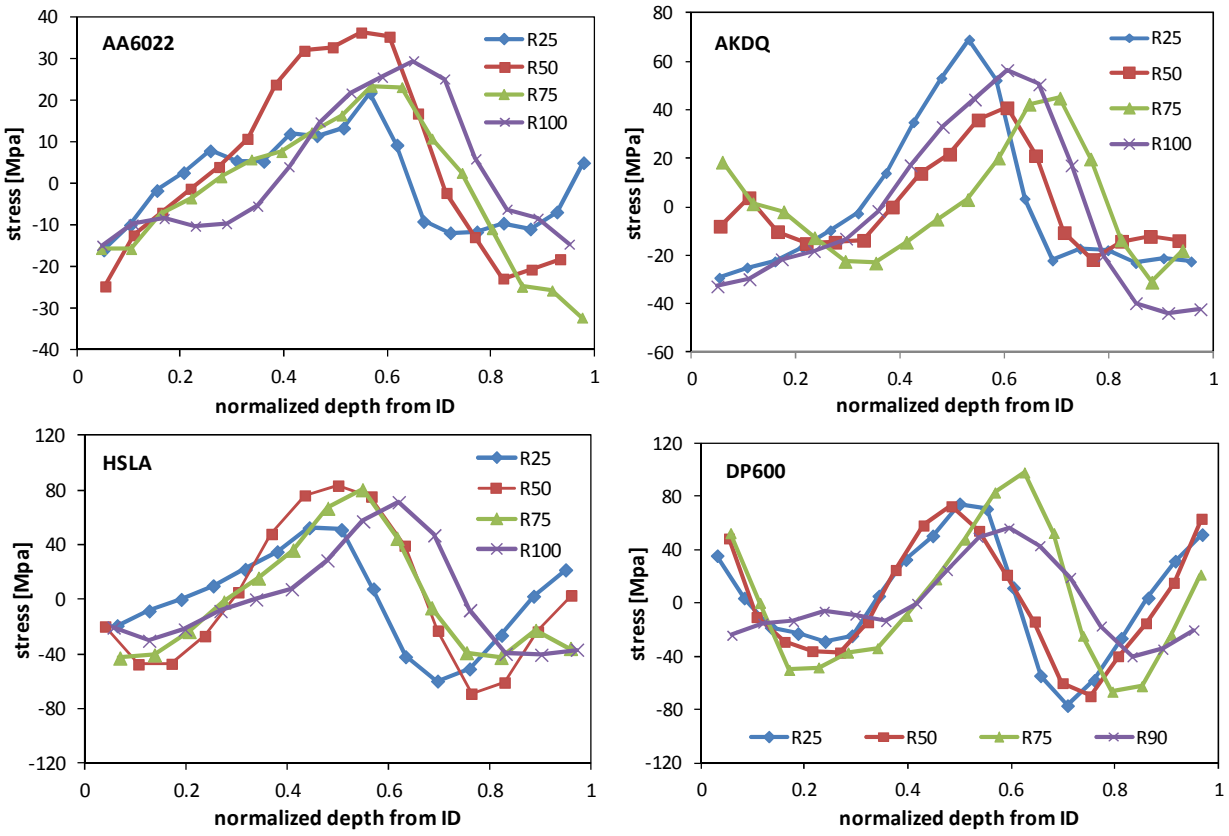

Figure 8. Normalized through-thickness stresses in AA6022 (top left), AKDQ (top right), HSLA50 (bottom left) and DP600 (bottom right). Increasing depth values go from intrados (ID) to extrados (Figure 1. 1). On average, one standard deviation for AA6022: 4 MPa; AKDQ: 8 MPa; HSLA: 10 MPa; and DP600: 12 MPa.

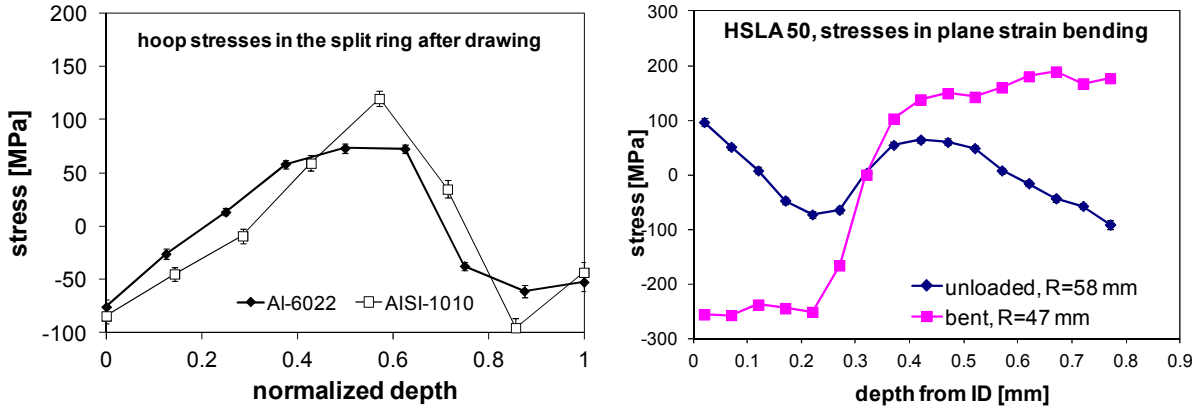

Figure 9. Through-thickness residual stresses from forming involving bending. Left: hoop stresses in split rings extracted from a deep drawn cup (AA6022: [4], AISI 1010 : [2]). Right: plane strain bending of HSLA 50 without stretching showing stresses in the bent and unloaded state.

A closer comparison of the stresses in Fig. 8 shows that the lowest and highest stress values for each material increase with the respective yield strength (AA6022: 132MPa; AQDQ: 163 MPa; HSLA50: 406 MPa; DP600: 424 MPa). Furthermore, the relative depth at which stresses change the sign from compressive to tensile (and vice versa) increases with penetration depth of the draw bean. In other words, with increasing elongation (ε_{major} increases with penetration) the neutral plane is shifted more in the direction intrados $\Rightarrow$ extrados). On the other hand, the shift of the neutral plane reduces springback and sidewall curl as reported in [1] (see Fig. 1).

Summary

The results of a study on through thickness residual stresses from a plane strain channel draw were presented. It was found that the general outline of the stress distributions is determined by the bending common to all samples. The effect of increasing draw bead penetrations is a shift of the entire stress distribution towards extrados. This finding was interpreted as the effect of the shift of the neutral plane.

References

[1] D.E. Green, T.B. Stoughton, T. Gnaeupel-Herold, M.A. Iadicola, T.Foecke, Influence of drawbeads in deep drawing of plane-strain channel sections, Proceedings of the IDDRG 2006 Conference, Porto, Portugal (2006) 559-566

[2] T. Gnaeupel-Herold, T.J. Foecke, H.J. Prask, R.J. Fields, An Investigation of Springback Stresses in an AISI-1010 Deep Drawn Cup, Mater. Sci. Eng. A399 (2005) 26-32

[3] T. Gnaeupel-Herold, M.A. Iadicola, T. Foecke, Residual Stresses in Numisheet Benchmark 3 Panels, Proc. of the International Deep-Drawing Research Group Annual Conference (2009) 7-16

[4] T. Gnaeupel-Herold, H. J. Prask, R.J. Fields, T.J. Foecke, Z.C. Xia and U. Lienert, A Synchrotron Study of Residual Stresses in a Al6022 Deep Drawn Cup, Mater. Sci. Eng. A366 (2004) 104-113.

[5] T. Gnäupel-Herold, Formalism for the Determination of Intermediate Stress Gradients using X-ray Diffraction, J. Appl. Cryst. 42 (2009) 192–197

[6] M. A. Iadicola, T. Foecke, and T. B. Stoughton, Experimental Procedures and Results for Benchmark 3: Stage 2 Forming Process, Proceedings of Numisheet 2005, American Institute of Physics, CP778 Volume B (2005 905-915.

[7] M.C. Oliveira, A.J. Baptista, J.L. Alves, L.F. Menezes, D.E. Green, T. Gnaeupel-Herold, M.A. Iadicola, T. Foecke, T.B. Stoughton, Two Stage Forming: Experimental and FE Analysis, Proceedings of IDDRG, June 2006, Porto (Portugal) 279-286

[8] T. Gnäupel-Herold, A.A. Creuziger, M.A. Iadicola, (2012), "A model for calculating diffraction elastic constants", J. Appl. Cryst. 45 (2012) 197-206

[9] T. Gnäupel-Herold, IsoDEC: A software for calculating diffraction elastic constants, J. Appl. Cryst. 45 (2012) 573-574

[10] T. Foecke,T. Gnaupel-Herold, Robustness of the Sheet Metal Springback Cup Test, Metallurgical and Materials Transactions A 37 (2006) 3503-3510

International Conference on Residual Stresses 9 (ICRS 9)
10.4028/www.scientific.net/MSF.768-769

Through-Thickness Stresses in Automotive Sheet Metal after Plane Strain Channel Draw
10.4028/www.scientific.net/MSF.768-769.433